Accepted Manuscript

Black-silicon production process by CF_4/H_2 plasma

E. Vassallo, M. Pedroni, S.M. Pietralunga, R. Caniello, A. Cremona, F. Di Fonzo, F. Ghezzi, F. Inzoli, G. Monteleone, G. Nava, V. Spampinato, A. Tagliaferri, M. Zani

PII: S0040-6090(16)00097-3
DOI: doi: 10.1016/j.tsf.2016.02.008
Reference: TSF 35007

To appear in: *Thin Solid Films*

Received date: 1 October 2015
Revised date: 1 February 2016
Accepted date: 4 February 2016

Please cite this article as: E. Vassallo, M. Pedroni, S.M. Pietralunga, R. Caniello, A. Cremona, F. Di Fonzo, F. Ghezzi, F. Inzoli, G. Monteleone, G. Nava, V. Spampinato, A. Tagliaferri, M. Zani, Black-silicon production process by CF_4/H_2 plasma, *Thin Solid Films* (2016), doi: 10.1016/j.tsf.2016.02.008

This is a PDF file of an unedited manuscript that has been accepted for publication. As a service to our customers we are providing this early version of the manuscript. The manuscript will undergo copyediting, typesetting, and review of the resulting proof before it is published in its final form. Please note that during the production process errors may be discovered which could affect the content, and all legal disclaimers that apply to the journal pertain.

ACCEPTED MANUSCRIPT

Black-silicon production process by CF_4/H_2 plasma

E. Vassallo[1*], M. Pedroni[1], S. M. Pietralunga[2,4], R. Caniello[1], A. Cremona[1], F. Di Fonzo[4], F. Ghezzi[1], F. Inzoli[1], G. Monteleone[2], G. Nava[4], V. Spampinato[1], A. Tagliaferri[3,4], M. Zani[3]

[1]CNR, Istituto di Fisica del Plasma "P. Caldirola", Via R. Cozzi 53, 20125 Milano, Italy

[2]CNR, Istituto di Fotonica e nanotecnologie, P.zza Leonardo da Vinci 32, 20133 Milan, Italy

[3]Politecnico di Milano, Dip. Fisica, P.zza Leonardo da Vinci 32 , 20133 Milan, Italy

[4]Center for Nano Science and Technology @PoliMi, Istituto Italiano di Tecnologia, Via G. Pascoli, 70/3, 20133 Milano, Italy

Abstract

Nanoscale structures in silicon have been produced by means of a maskless plasma process that employs tetrafluoromethane and hydrogen. The influence of the radio-frequency power and process time on the surface texturing was studied. Desirable texturing effect has been achieved by applying an RF power in the range of 200-280 W and process time in the range of 20-30 min. The textured surface is characterized by nanopillars with lateral dimensions ranging from 50 to 300 nm and with a depth in the 100-300 nm range. Depending on process parameters in the plasma etching recipe, the optical reflectance of the silicon surface is lowered and R < 5 % is reached in the range going from the visible to the near-IR region.

Keywords: Plasma process, Reactive ion etching, Reflectance, Solar cells, Silicon surface texturing

1 Introduction

The physical structuring of silicon is one of the cornerstones of modern microelectronics and integrated circuits. Regarding Silicon-based optical detectors and solar cells, the high reflectivity at input surface can hinder efficient light collection. Surface texturing is one way to minimize unwanted reflections and lately, the anti-reflection effect of the Si surface texturization has been

* Corresponding author. Tel.: +39 2 66173245; fax: +39 2 66173203.
E-mail address: vassallo@ifp.cnr.it (Espedito Vassallo).

ACCEPTED MANUSCRIPT

particularly studied in view of light absorption enhancement in solar cells [1-4]. The texturing of the Si surface was also proved to be effective in functionalizing it as a scaffold for biomedical applications, by providing selective antibacterial characteristics [5]. In these fields of application, the realization of high-aspect-ratio vertical features on Si substrates is the crucial step in the fabrication process. For this purpose, laser-based manufacturing processes have been proposed and developed [2, 6]; wet chemical etchants can also be exploited to create anisotropic profiles, because they are cost-effective and easy to use, but not environmentally friendly. The use of dry processes instead of wet has been strongly supported in recent years, and dry plasma etching has become a conventional technology in microelectronics. In particular, halogen-based plasmas have been extensively used for Si etching. What is usually seen as an undesirable effect in plasma etching is surface roughening, which can usefully be controlled to induce Si texturing under certain experimental conditions. The Si texturization has been studied mainly in fluorine-based plasmas by exploiting the random automasking effect on surface during the etching. It has been demonstrated that the automasking effect is obtained if a random passivation is generated during the etching [7]. The passivation is essential for protection of sidewalls and obtaining vertical features. C_4F_8 gas has been used as the reactant to produce a polymeric passivation layer which protects the trench sidewalls realized in the etching process by fluorine based gas such as SF_6 [8-9]. Maruyama et al. reported a texturization process which employed SF_6 plasma in the etching process and a mixture of O_2 gas during the passivation step [10]. It is worth mentioning that the latest process exploits a low-density plasma power and no polymeric passivation is needed, instead a growing SiO_xF_y layer is formed during the passivation step. In this paper, we report on the development of a method, based on hydrogen in place of oxygen, for the formation of the passivation layer. The purpose of this research is the fabrication of nano-structures on Si substrates, to be used either to enhance light absorption for opto-electronics and photovoltaic applications, or to provide patterned surfaces for bio-medical applications. The process is realized in a low-density capacitively-coupled plasma RIE reactor in CF_4 /H_2 mixture.

ACCEPTED MANUSCRIPT

ACCEPTED MANUSCRIPT

2 Experimental

2.1 The plasma reactor

An RF plasma system [11] has been used to produce a physical structuring of Silicon (type P, dopant B, <100>, 0.01-0.02 Ohm-cm, 1×1 cm^2, thickness = 400 μm). The experimental apparatus consists of a parallel-plate, capacitive-coupled system, consisting of a cylindrical stainless steel vacuum chamber with an asymmetric electrode configuration. A powered electrode (3-in diameter) is connected to an RF (13.56 MHz) power supply, coupled with an automatic impedance matching unit, while the other electrode (3-in diameter), consisting of stainless steel, is grounded. Si substrates are placed on the powered electrode at 6 cm away from the ground electrode. The substrate temperature is monitored by a thermocouple fixed directly on the substrate. Before the process, the substrates are cleaned by chemical etching solutions (alcohol followed by rinse in deionized water) to remove surface contaminants. The Atomic Force Microscopy technique has been used to check the surface roughness of substrates after cleaning. The RMS roughness was in accordance to manufacturer's data (≤ 1 nm). The process chamber is pumped to a base pressure below 1×10^{-5} Pa and high-purity reactive gases (CF_4 and H_2) are introduced into the vacuum chamber through a mass flow controller in order to establish the desired working pressure, which is fixed at 1×10^{-3} Pa. The plasma phase has been characterized through optical emission spectroscopy. The experimental apparatus consists of a scanning monochromator (Horiba JobinYvon iHR550) of the Czerny–Turner type, with a focal length of 0.55 m, built around a holographic diffraction grating with 1800 grooves/mm, coupled with a CCD (Synapse Horiba JobinYvon) camera, thermoelectrically cooled to -70 °C. The optical emission from the plasma is collected from the bulk volume of the discharge through a quartz window by a plane-convex convergent lens of 1 inch. diameter and conveyed by an optical fiber (length 3 m, core 600 mm, numerical aperture 0.22) onto the entrance slit of the monochromator, keeping the slit aperture fixed at 50 μm.

ACCEPTED MANUSCRIPT

2.2 *Coatings characterization*

The nano-structured samples have been characterized for their total optical reflectance (sum of normal and diffuse reflectance) in the spectral range 250-1100 nm by means of a spectrophotometer (Perkin Elmer LAMBDA 1050 UV/Vis/NIR), equipped with a 150 mm diameter integrating sphere.

Different surface analysis methods were performed to investigate the morphology and chemical properties of the nano-textured samples. HI-resolution SEM imaging was performed using a Tescan MIRA III Field-Effect SEM. The surface chemical characterization was carried out by means of X-ray photoelectron spectroscopy (XPS). The core level spectra were acquired using a non-monochromatized Al anode X-ray source ($h\nu$ = 1486.6 eV) VSW model TA10 and a hemispherical analyzer VSW model CLASS 100, equipped with a single channel detector, operating in constant pass Energy mode (22 eV) with 0.9 eV of overall resolution. Wide scan spectra were acquired with 2 eV of overall resolution. All spectra were referenced to the same energy scale determined by calibrating the Ag 3d5/2 line at 368.3 eV. In order to clarify the formation mechanism of nanostructures on Si surface, Scanning Auger Micro-spectroscopy (SAM) was used to complement XPS analysis. The purpose is to provide additional information about the selective etching process by locally measuring the elemental composition in different spots of the textured surface. Auger electron spectroscopy probes the elemental composition of surface layers, as well as interfaces and grain borders, down to a depth of about 1÷2 nm with a sensitivity of about 1% at., while the lateral resolution is set by the diameter of the electron beam [12]. In the present work, the SAM system (PHI 660) was operated at e-beam acceleration voltage V=10 kV, e-beam current I=32 nA and analyzer energy resolution $\Delta E/E$=0.5%.

ACCEPTED MANUSCRIPT

3 Results and discussion

3.1 Texturing process development

Under suitable plasma conditions [13-14], the fluorocarbon molecules undergo fragmentation and ionization, and the main species produced are CF_x and F, of which the most useful to the purpose is the Fluorine species. When an F atom hits the substrate, it can remove a Si atom. By chemical reaction of F with Si, a volatile SiF_4 gas is created and then pumped out of the chamber. The etching is predominately a chemical etching, so the control of the F density in chamber strongly affects the etching rate. The main parameters to control the F density include RF power, gas flow rate, pressure and different dilution of gases. In order to tune the texturization process based on the hydrogen content, we have rated the fabrication of nano-structures as a function of RF power and gas concentration. As is well-known [15], the fragmentation and ionization processes of the molecules are increased as the RF power increases. This means that the density of F atoms and the etching rate increase as a function of power (Fig. 1-2). Fig. 2 shows the collected emission by OES of main $3s^2P$ (703.7 nm) fluorine line [16] as a function of H_2 concentration and RF Power. A strong correlation between the etching rate and F density as a function of RF power was found (Fig. 1). OES results also show that the atomic fluorine concentration in CF_4 plasma increases as a function of H_2 concentration (Fig. 2).

ACCEPTED MANUSCRIPT

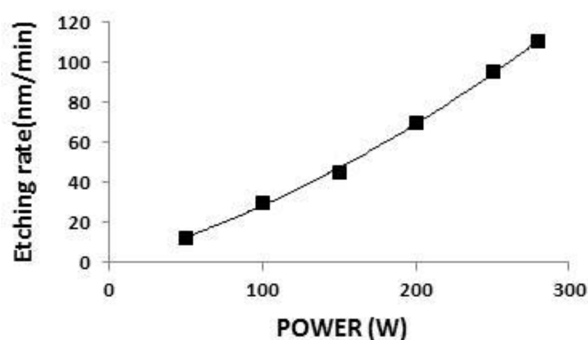

Fig. 1. Etching rate as a function of RF power in H_2/CF_4 plasma with 2 sccm of H_2 dilution (Etching time 10 min)

ACCEPTED MANUSCRIPT

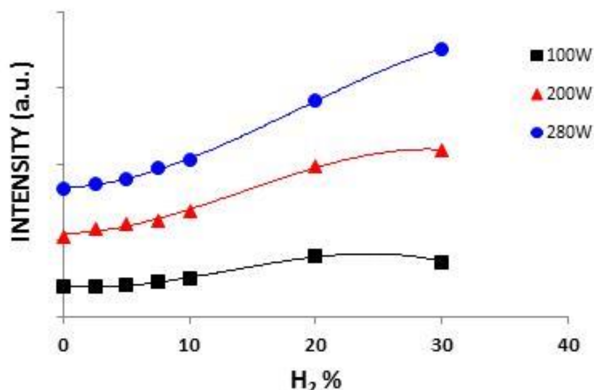

Fig. 2. OES atomic fluorine emission versus H_2 concentration for different values of RF power

The fluorine emission trend reported in the Fig. 2 may seem in contradiction with the well-known process that involves the recombination of H with F to form HF, thus resulting in a decrease of the F concentration as hydrogen concentration increases [17]. However, the addition of H_2 also simultaneously plays an important role in the fragmentation of CF_4 [18], generating a higher density of F radicals. Actually, at small amounts of H_2 the fragmentation process predominates over the recombination. Fig. 3 shows the Si etching rates at 200 W (4.3 W/cm^2) of power applied to RF electrode, as a function of the H_2 concentration in the feed gas. After an initial increase, the etching rate decreases at H_2 percentages higher than ≈ 5 %. At first sight, this could be in contrast with the rationale given for Fig. 2, where the intensity of F radical monotonically grows with the increase in hydrogen concentration. However, the trend observed in Fig. 3 can be explained by considering that the etching rate of Si in fluorocarbon plasmas depends on the competition between the etching itself, due to the action of fluorine, and the deposition of CF_x radicals onto the surface. Therefore, the action of the H_2 concentration on the kinetics of the overall process can be synthesized by plotting the ratio of F/CF_x intensity, as determined by the OES signals vs. H_2 concentration (Fig. 3, right).

ACCEPTED MANUSCRIPT

ACCEPTED MANUSCRIPT

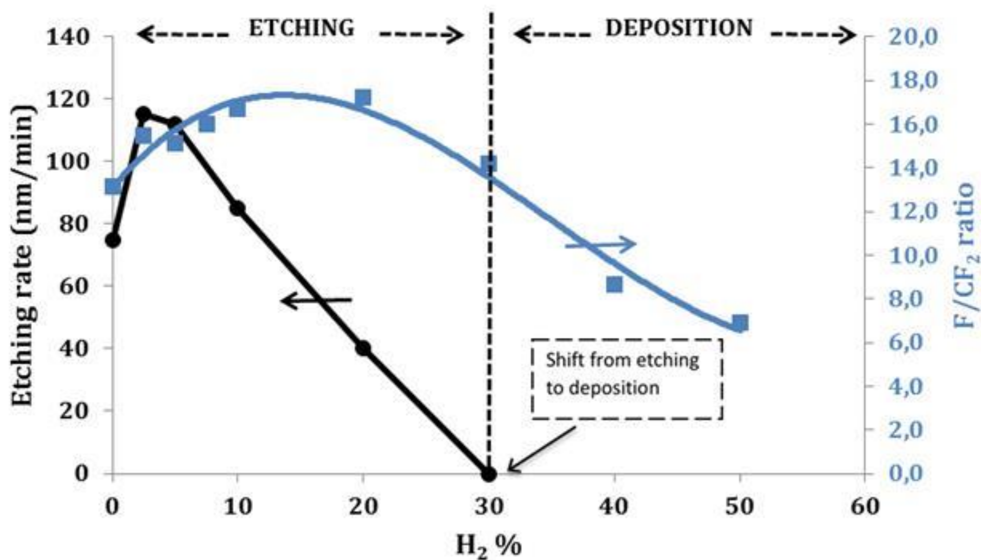

Fig. 3. Etching rates of Si and F/CF_2 ratio evaluated by OES as a function of the H_2 concentration in the feed gas (Treatment time 10 min, RF power200 W)

Namely, CF_2 is used as a representative radical for deposition [19]. The F/CF_2 ratio gradually increases with increasing H_2 content until the latter reached ≈10%, and then it monotonically decreases. The measured trend of the F/CF_2 ratio and the measured trend of the etching rate both show a similar behavior as a function of H_2 concentration, as shown in Fig. 3. Moreover, the maximum for the etching rate and the maximum of the F/CF_2 ratio approximately correspond both to a Hydrogen concentration of ≈ 10% H_2.

Beyond the main etching process, at the same time, a passivation layer can be created with H particles, CF_x radicals and the partially etched product SiF_x. In certain experimental conditions, the recombination of these particles can become energetically favorable and a thin layer can be created. This thin film acts as a thin protection layer from etching. At the beginning of the process the passivation layer which mainly consists of SiH_x, Si-F_x and SiC_xF_y bonds, starts to form on the surface of the sample in random way. An automask on the Si surface is generated. The mask material is a nonvolatile by-product of interaction between plasma and surface. Simultaneously ion

ACCEPTED MANUSCRIPT

bombardment casually removes a part of the passivation layer formed. Passivated and etched areas will be etched with different rates and therefore anisotropic etching predominates and a black silicon can be formed.

For better understanding of the texturing, we have also checked possible metal aggregates sputtered from the target that can act as micromask [20]. XPS analysis was carried out on our samples. No metal was found (XPS detection limit ≈ 1%), therefore, the contribution of the sputtered material to the automasking process can be considered negligible.

Regarding the texturing process, H_2 concentration in CF_4 plasma is fundamental to control the anisotropic nature of the etching process. A low concentration of H_2 implies a too strong etching, since the passivation layer will not have enough atoms to act as a protective layer. Vice versa, too much H_2 shifts the process from etching to deposition (Fig. 3) and the anisotropic nature of the etching is lost. In the present study, the effect of H_2 concentration in the mixture is evaluated by SEM (not shown). In order to have a predominant effect of the anisotropic etching a low H_2 concentration is required, hence the optimum H_2/CF_4 ratio of about 0.1 was chosen. Since the passivation layer may be thermally unstable, in order to avoid the use of expensive coolers, a study of the temperature of the sample holder as a function of RF power was performed. After verifying that the temperature of the specimen exceeds 100°C at RF power above 300 W (6.5 W/cm^2), we limited our study to RF values up to 280 W (6.1 W/cm^2). At 200 W (4.3 W/cm^2) of RF Power and H_2/CF_4 ratio equal to 0.1. The evolution of the height of nano-structures as a function of different values of the process time was assessed by SEM (Fig. 4). At times less than 10 min the competition between the etching and texturing processes is unbalanced towards etching, so an insufficient texturing is formed. A good texturing is reached for times ranging from 10 to 30 min: for higher times the height of obtained structures decreases. This effect could be attributed to deterioration of the passivation layer due to the increase of the sample holder temperature. Therefore a process time in the range of 10-30 min was chosen.

ACCEPTED MANUSCRIPT

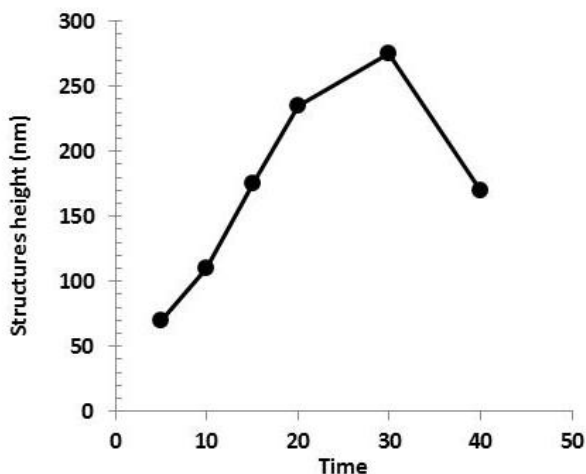

Fig. 4. Evolution of height of structures as a function of process time (200 W, H_2/ CF_4=0.1).

3.2 Morphological and optical properties

The surface morphology of Si specimens processed by plasma (at H_2/CF_4 ratio 0.1) for RF powers in the range of 200-280 W and treatment time of 20 min is shown in the SEM images in Fig. 5. All treated Si samples showed a black surface, when seen in white light. The top-view SEM micrographs of the Si etched surfaces are shown in Fig. 5a-c. Looking at the cross-sectional view (Fig. 5d) it resembles a pattern of spaced vertical nanopillars of 150-200 nm diameters separated by 100-150 nm. Instead, the top view shows only a few nanopillars and the formation of random nanostructures on the surface of processed substrate is evident. The increase of RF power (Fig. 5a-c) slightly enhances the numbers of nanopillars.

ACCEPTED MANUSCRIPT

ACCEPTED MANUSCRIPT

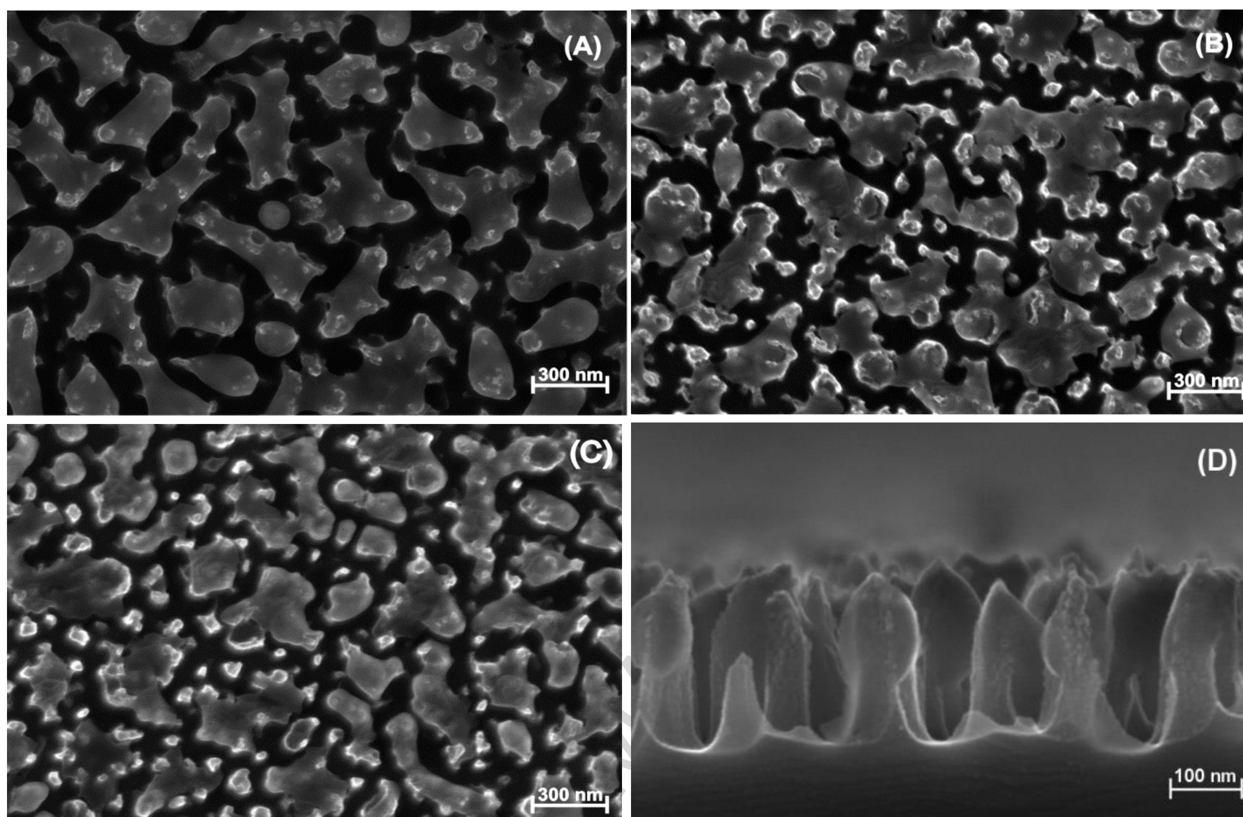

Fig. 5. SEM pictures of Si wafers etched as a function of RF Power: (a) 200 W, (b) 250W, (c) 280 W, (d) cross-sectional view at 200 W.

The black Si surface was characterized in the visible to IR spectral region using a UV-VIS spectrophotometer. Fig. 6 shows the total reflectance spectra (sum of normal and diffuse reflectance) of the textured Si produced with H_2/CF_4 ratio 0.1 as a function of RF power (200-280 W) with a treatment time fixed at 20 min. The reflectance of the untextured Si is plotted for comparison (Fig. 6A). For all treated samples, the Si surface shows (Fig. 6B) a very low reflection in the visible as well as in the near-IR regions and optical reflectance is kept below 10%. No substantial difference as a function of RF power is found in the range 200-280 W (4.3-6.1 W/cm^2). Samples etched at power lower than 200 W (4.3 W/cm^2) were also analyzed, showing a substantial increase in reflection. Therefore subsequent discussion is focused on experimental condition that led to reflectance below 10 %.

ACCEPTED MANUSCRIPT

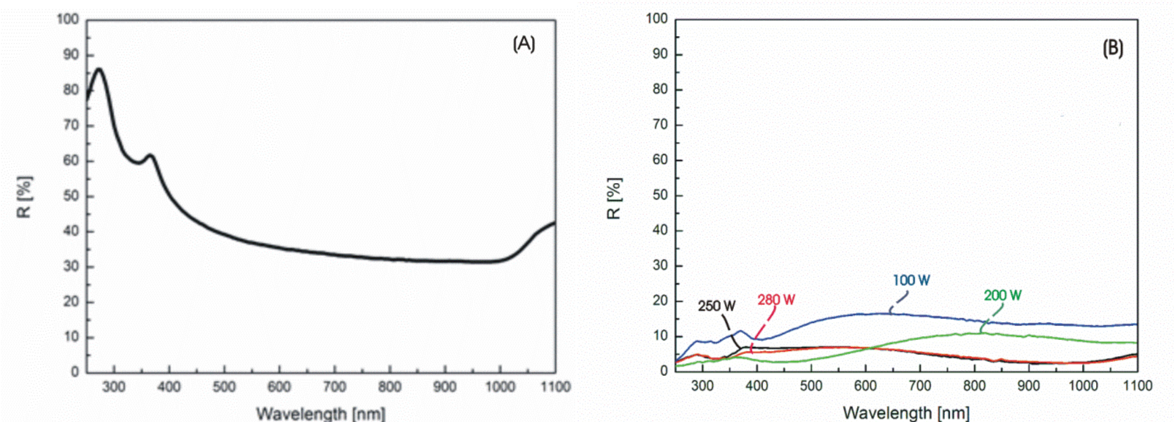

Fig. 6. Spectral reflectance of reference Si wafer (A) and of textured Si (B) as a function of RF power.

Regarding the morphology, we observed a slight increase in the numbers of nanopillars, as RF power is raised above 200 W (Fig. 5b-c). However, this does not seem to affect the spectral reflectance below 600 nm. It is worth noting, nevertheless, that in the case of RF = 200 W(4.3 W/cm^2), where the nanopillars are fewer and less sharp than in the case 250 W and 280 W, the spectral reflectance above 600 nm slightly worsens. SEM investigation was also performed as a function of the treatment time. SEM micrographs of the Si etched surfaces at 200 W (4.3 W/cm^2) of RF power, with H_2/CF_4 ratio of 0.1, are shown in Fig. 7. The following aspects can be noted with regard to the nanostructures: a slight increase in the number of nanopillars and a strong increase of nanopillars height as a function of time.

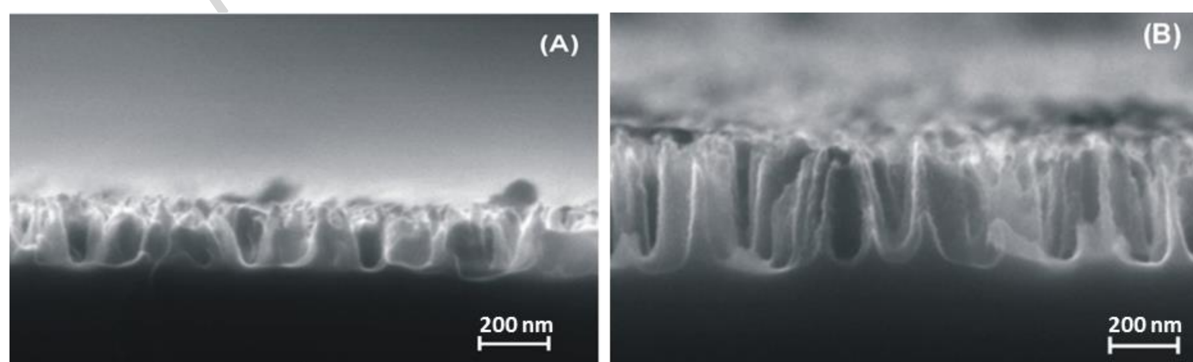

Fig. 7. SEM cross-sectional pictures of Si wafers etched at 200 W as a function of treatment time: (A) 10 min, (B) 30 min.

ACCEPTED MANUSCRIPT

The spectral reflectance of the textured Si produced with H_2/CF_4 ratio 0.1, at 200 W (4.3 W/cm^2) of RF power is shown in Fig. 8, as a function of the process time (from 10 to 30 min). In this case, also, the Si surface shows for all samples a low reflection in the visible as well as in the near-IR region in comparison with bulk Si. Nevertheless, we notice that, by shortening the process time to 10 min, the spectral reflectance above 700 nm worsens. The best optical reflectance performance, for samples textured at treatment times longer than 20 min, could be justified by the optical trapping effect induces by both the higher number of nanopillars and their increased height. Indeed, the incident light on the Si wafer is partially absorbed and reflected, and then the reflected light can penetrate the neighboring nanopillars, producing a strong trapping effect. Therefore, more nanopillars increase the light trapping reducing the total reflectance [Brian et al. ref 6].

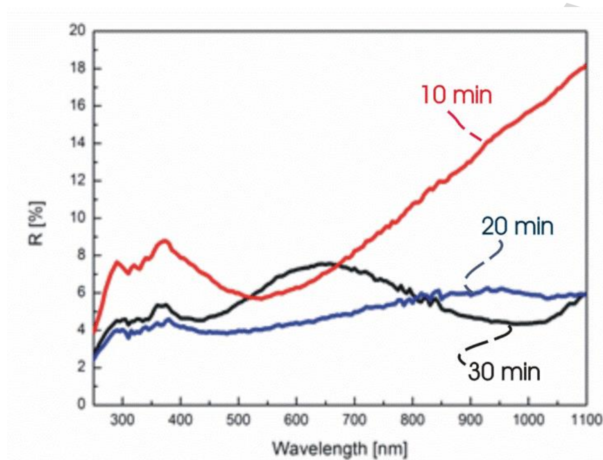

Fig. 8. Spectral reflectance of textured Si as a function of the process time.

3.3 Surface characterization

In order to study the nature of the passivation layer on the surface of the Si samples, XPS depth profiles, via 3 keVAr^+ sputtering, on samples deposited with three RF powers were carried out. The total erosion depths were measured with a Tencor P15 profilometer and, in turn, the sputtering velocity was simply calculated dividing the eroded depth by the erosion time. Survey scans were carried out at each layer at the highest sensitivity in order to reveal the appearance of new elements. The main elements detected are C, F, Si and O. The chemical characterization of these elements

ACCEPTED MANUSCRIPT

was carried out via high resolution core level spectra (1.35 eV). Survey and high resolution spectra have been acquired with a 5 nm stepwise. These spectra were DECONVOLUTED to obtain information on the chemical species deposited. We report, as example, in (Fig. 9) the results of the deconvolution for the C_{1s} and Si_{2p} at the surface for the sample obtained at 200 W (4.3 W/cm^2). As can be noticed from the C_{1S} line, the presence of the C-F bonds is typical of those for a fluoropolymer [21]. C-O-Si type bonds are also found in literature while the C-C bond at 284.6 eV of binding energy is assigned to the adventitious carbon. On the other hand, the Si-F bonds found under the Si_{2P} LINE ARE TYPICAL FOR SI ETCHED BY F WHILE SiO_2 BOND IS DUE TO THE PRESENCE OF OXYGEN IN THE PLASMA DURING THE PROCESS. Depth profiles are not presented here since a dedicated study to investigate about the growth of the structures is in progress. We noticed the progressive disappearing of the CF_2, CF_3, SiO_2 and SiF_3 with depth. XPS measurements confirmed the presence of the expected passivation layer. It is shown that these layers are mainly composed of CF_x and SiF_x components.

ACCEPTED MANUSCRIPT

ACCEPTED MANUSCRIPT

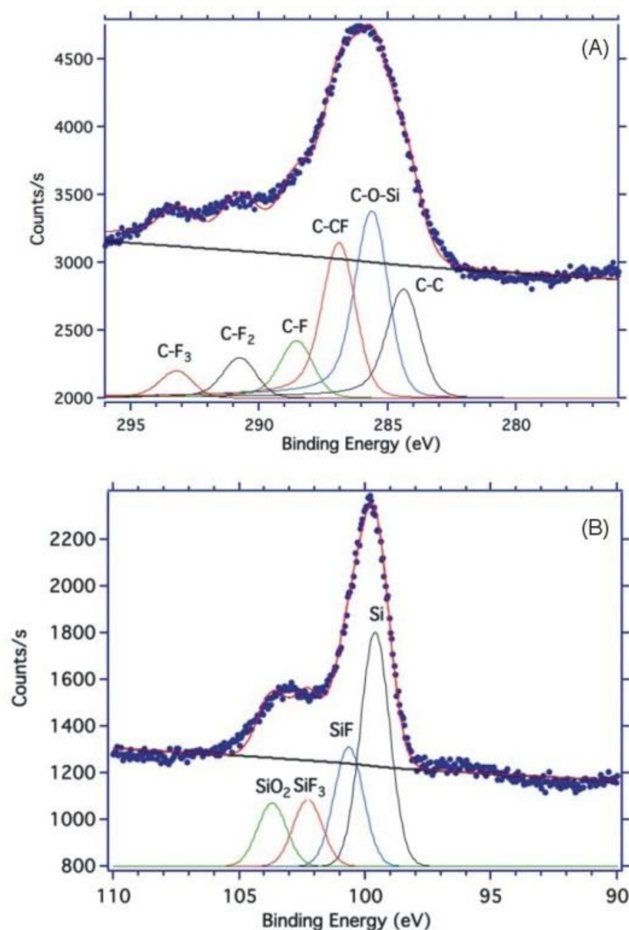

Fig. 9. $C_{1s}$and Si_{2P} high resolution spectra at the surface for the 200 W sample.

SAM analysis was performed on sample regions as those in the SEM image of Figure 10 (left). On this sample, we identified some areas with defective nano-texturing. In the regions where the pillars were evenly distributed, Auger spectra were taken on areas 1 x 1 um^2 wide, both at normal e-beam incidence and at 20 deg of sample tilt. By probing the samples at normal incidence, signal contributions from the top of the pillars as well as from the Silicon wafer at bottom are expected; however, Auger signal from the Si at bottom is expected to suffer from a strong attenuation, because of the morphology of the black silicon layer. In fact, the high aspect ratio of the pillars is expected to contribute for a reduction in the yield of Auger electrons emitted at the bottom of the trenches [22]. By tilting the samples, the lateral surface and top of pillars are probed, to identify the composition of the passivating capping layer of pillars.

ACCEPTED MANUSCRIPT

Auger differentiated survey spectra taken from various areas at the surface of textured sample are compared in Figure 11. Plots are statistically representative of the system under test, meaning that spectra taken at areas of similar morphology on the sample are fully equivalent. As for XPS characterization, detected elements are C, Si, O and F. The presence of Silicon at surface is identified by the two Silicon spectral peaks Si(KLL) at E=1621 eV and Si(LMM) at E=96 eV. Oxygen is identified by O (KLL) peak at E= 510 eV. The presence of Carbon is identified by the Auger C (KLL) peak at E=275 eV. It is worth saying that samples have not been ion-beam sputtered, prior to SAM analysis, avoiding changes in the structure of the capping layer at the surface of pillars. Specifically, this means that contamination by Carbon and by Oxygen is generally evenly present and that, consequently, the Fluorine peak F(KLL) at E=659 eV has been used as the local marker for the distribution of the fluorinated passivating layer.

SAM characterization on the lateral surface and top of etched pillars is expressed by line (a). SAM spectrum definitely marks the presence of Fluorine atoms and a high quantity of Carbon, both of which are constituents of the passivating layer; the Si peaks are strongly attenuated, fact that is consistent with the presence of Carbon at the surface. Spectrum (a) markedly differs from Auger spectrum (b), which expresses the local elemental composition of the Silicon surface, at the bottom of pillars. The most distinguishing feature is the negligible Fluorine content, comparable with noise level, and the clear increase in Si peak. SAM results are therefore consistent with the presence of the passivating capping layer on the top and along the walls of etched pillars, while they clearly state the absence of such layer at the bottom of the Black Silicon surface.

ACCEPTED MANUSCRIPT

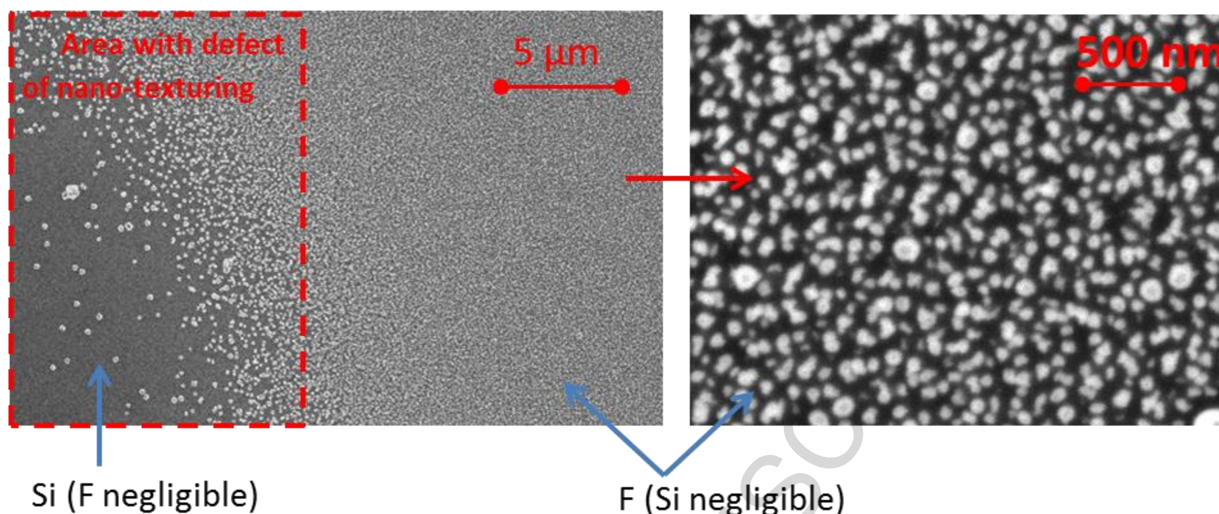

Fig. 10. SEM top pictures (left) of Si wafers etched at 100 W, (right) magnification of area with pillars.

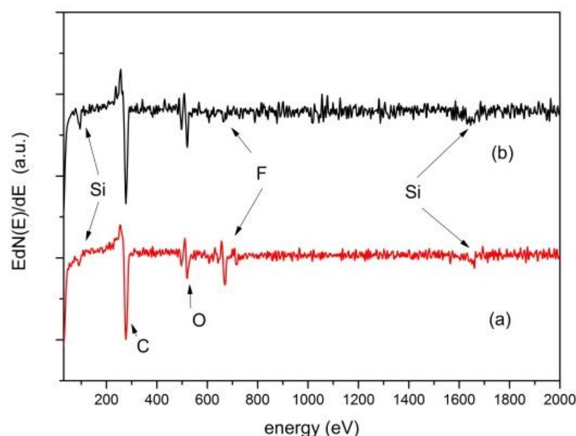

Fig. 11. Scanning Auger spectra in Black Silicon, showing local elemental composition at textured surface: (a) SAM spectrum from the surface of etched pillars (average on 1x1 μm^2 area); (b) SAM spectrum obtained from the bottom surface of Silicon.

4. Conclusion

Random nanoscale structures were fabricated in a capacitive coupled plasma reactor by using a CF_4/H_2 plasma, at a process temperature below100°C, without using any masks. The effects of plasma parameters such as RF power, H_2 concentration and process time were studied. According to the experiments performed in this study, a RF power in the range 250-280 W (5.5-6.3 W/cm^2), an

ACCEPTED MANUSCRIPT

H_2/CF_4 ratio of 0.1 and a process time in the range 20-30 min could be an optimal condition to produce a nanostructured Si surface featuring an optical reflectance below 5 % in the visible range. The possibility of fabricating nanostructured Si without the use of lithography offers an interesting low-cost process for innovative optoelectronic devices and also in view of biomedical applications.

Acknowledgements

This work was supported within the CNR-Regione Lombardia agreement n° *18088/RCC,* August 5th *2013* and within the CNR-Regione Lombardia framework agreement, Decr. Reg. n. 3667 - 29/04/2013.

References

[1] P. Campbell, M.A. Green, Light trapping properties of pyramidally textured surfaces, J. Appl. Phys. 62 (1987) 243.

[2] E. Mazuret al., Systems and methods for light absorption and field emission using microsctructured silicon, US Patent 7,390,689 B2(2008).

[3] J.S. Yoo, I.O. Parm, U. Gangopadhyay, Kyunghae Kim, S.K. Dhungel, D. Mangalaraj, Junsin Yi, Black silicon layer formation for application in solar cells, Solar Energy Materials & Solar Cells 90 (2006) 3085-3093

[4] S.Q. Xiao, S. Xu, High-efficiency Silicon Solar Cells-Materials and Devices Physics, Critical Reviews in Solid State and Materials Sciences, 2014, 39, 277-317

[5] E. P. Ivanova et al. , Bactericidal activity of black silicon, Nature Communications 4:2838 DOI:10.1038/ncomms3838 (2013).

[6] Brian R. Tull,James E. Carey, Eric Mazur, Joel P. McDonald, Steven M. Yalisove, Silicon Surface Morphologies after Femtosecond Laser Irradiation,MRS Bulletin. 2006; 31(8):626-633.

ACCEPTED MANUSCRIPT

ACCEPTED MANUSCRIPT

[7] S Kalem, P Werner, Ö Arthursson, V Talalaev, B Nilsson, M Hagberg, H Frederiksen and U Södervall, Black silicon with high density and high aspect ratio nanowhiskers, Nanotechnology 22 (2011) 235307.

[8] Laermer F and Schilp A, Method of anisotropically etching silicon US Patent 5,501,893A (1996).

[9] S.Q. Xiao, S. Xu, K.Ostrikov, Low-temperature plasma processing for Si photovoltaics, Materials Science and Engineering R-Reports 2014, 78 (1), 1-29

[10] Maruyama T, Narukage T, Onuki R and Fujiwara N, High-aspect-ratio deep Si etching in SF6/O_2 plasma. II. Mechanism of lateral etching in high-aspect-ratio features, J. Vac. Sci. Technol. B 28 862 (2010)

[11] H.R. Koenig, L.I. Maissel, IBM J. Res. Dev. 14 (1970) 168.

[12] W. Metaferia, Yan-Ting Sun, S. M. Pietralunga, M. Zani, A. Tagliaferri and S. Lourdudoss, Polycrystalline InP on Si by using In metal assisted growth in hydride vapor phase epitaxy, J. Appl. Phys. 116 (3) 33519 (2014).

[13] W. W. Stoffels, E. Stoffels, and K. Tachibana, Polymerization of fluorocarbons in reactive ion etching plasmas, J. Vac. Sci. Technol. A, Vol. 16, No. 1, Jan/Feb (1998)

[14] Jean-Paul Booth, Optical and electrical diagnostics of fluorocarbon plasma etching processes, Plasma Sources Sci. Technol. 8 249 (1999)

[15] V. M. Donnelly and A. Kornblit, Plasma etching: Yesterday, today, and tomorrow, J. Vac. Sci. Technol. A 31(5), Sep/Oct (2013) 050825-1

[16] J. P. Booth and N. Sadeghi, Oxygen and fluorine atom kinetics in electron cyclotron resonance plasmas by time-resolved actinometry, J. Appl. Phys. 70, 611 (1991)

[17] Denise C. Marra and Eray S. Aydil, Effect of H_2 addition on surface reactions during CF4/H2 plasma etching of silicon and silicon dioxide films, J. Vac. Sci. Technol.A 15(5)Sep/Oct (1997) 2508

ACCEPTED MANUSCRIPT

ACCEPTED MANUSCRIPT

[18] Yukinobu Hikosaka, Hirotaka Toyoda and Hideo Sugai, Drastic Change in CF_2 and CF_3 Kinetics Induced by Hydrogen Addition into CF_4 Etching Plasma, , Jpn. J. Appl. Phys. 32 L690 (1993)

[19] L. Martinů and H. Biederman, Monitoring the deposition process of metal-doped polymer films using optical emission spectroscopy, Plasma Chem. Plasma Process. Vol 5, No1(1985) 81-87

[20] M. Gharghi and S. Sivoththaman, Formation of nanoscale columnar structures in silicon by a maskless reactive ion etching process, J. Vac. Sci. Technol. A 24(3) May/Jun 2006, 723-727

[21] Y. Kim,Ji-Hye. Lee, Kang-Jin Kim, Y. Lee,Surface characterization of hydrophobic thin films deposited by inductively coupled and pulsed plasmas, J. Vac. Sci. Technol. A 27, 900(2009)

[22] M. Prutton, M. M. El-Gomati Eds., Scanning Auger Electron Microscopy, John Wiley & Sons, Ltd. ISBN: 0-470-86677-2 (2006)

ACCEPTED MANUSCRIPT

ACCEPTED MANUSCRIPT

Highlights

- Si texturing can be produced by a maskless plasma process.
- Si texturing can be tuned by changing plasma power and process time.
- Surface optical reflectance can be lowered to 5-10 % from visible to the near-infrared

ACCEPTED MANUSCRIPT